Journal of Physics: Conference Series

Wind tunnel experiments to prove a hydraulic passive torque control concept for variable speed wind turbines

To cite this article: N F B Diepeveen and A Jarquin-Laguna 2014 *J. Phys.: Conf. Ser.* **555** 012028

Wind tunnel experiments to prove a hydraulic passive torque control concept for variable speed wind turbines

N F B Diepeveen, A Jarquin-Laguna

Offshore Engineering Section, Delft University of Technology, Stevinweg 1, 2628 CN, Delft, The Netherlands

E-mail: n.f.b.diepeveen@tudelft.nl, a.jarquinlaguna@tudelft.nl

Abstract. In this paper the results are presented of experiments to prove an innovative concept for passive torque control of variable speed wind turbines using fluid power technology. It is demonstrated that by correctly configuring the hydraulic drive train, the wind turbine rotor operates at or near maximum aerodynamic efficiency for below rated wind speeds. The experiments with a small horizontal-axis wind turbine rotor, coupled to a hydraulic circuit, were conducted at the Open Jet Facility of the Delft University of Technology. In theory, the placement of a nozzle at the end of the hydraulic circuit causes the pressure and hence the rotor torque to increase quadratically with flow speed and hence rotation speed. The rotor torque is limited by a pressure relief valve. Results from the experiments proved the functionality of this passive speed control concept. By selecting the correct nozzle outlet area the rotor operates at or near the optimum tip speed ratio.

1. Introduction

1.1. Hydraulic power transmission concept

As an alternative to geared and direct drive solutions, fluid power drive trains are being developed by several institutions around the world. The main motivations for this are the relative compactness of hydraulic drives, the option of having variable transmission ratio and the capability to dampen the dynamic response of the rotor to turbulent wind loads [1]. Although regarded as less energy efficient, fluid power drive trains are seen by many [2, 3] as having great potential to reduce the cost of offshore wind energy.

The common configuration is to have a horizontal axis wind turbine rotor coupled to a hydraulic pump, which converts the low speed, high torque mechanical power of the rotor to a high pressure flow. A high pressure line connects the pump to a hydraulic motor where the pressurised flow is converted back to mechanical power. The motor is coupled to a synchronous generator and thus operating at constant speed. Variable speed operation is realized by changing the volumetric displacement of the motor, and thus the transmission ratio, through active control [2, 4]. However, this paper explores a different concept, which is presented in figure 1. Unlike the conventional hydrostatic transmission, the high pressure line connects the pump to a nozzle instead of a motor. The nozzle converts the high pressure and low speed flow into a high speed jet U_{jet}, i.e. hydrostatic to hydrodynamic power. Converting the power in the jet to electricity can be done using an impulse hydro turbine, such as a

Pelton turbine. This arrangement allows to have a physically decoupled system between the rotor-hydraulic transmission and the Pelton wheel-generator at the grid size. In this way, the operation of the rotor and hydraulic transmission is independent of the Pelton wheel and generator. Thus, the focus of this paper is only on the rotor and hydraulic transmission.

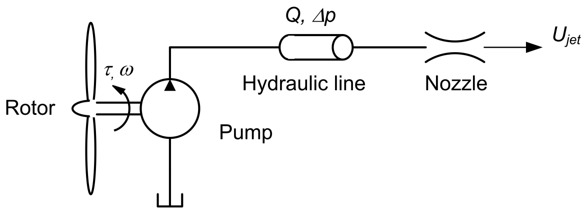

Figure 1. Simplified diagram of the proposed hydraulic transmission concept.

1.2. Passive torque control

The main idea behind the presented concept is to achieve a variable speed operation of the rotor without any form of active control. By sizing the nozzle area correctly, the torque-speed operation of the hydraulic transmission is closely matched with the ideal torque-speed operation of the rotor required for maximum aerodynamic performance. The rotation speed ω of the pump shaft creates a volumetric flow rate Q. The volumetric flow rate and the cross sectional area of the nozzle at the end of the circuit determine the pressure in the high pressure line. The pressure difference Δp over the pump is directly proportional to the torque transmitted by the pump τ. To avoid an overloading torque, the pressure at the pump is limited to a predetermined maximum by a pressure relief valve.

1.3. Objective: proof of concept through experimentation

The way to prove that this concept of passive torque control works in real life is through practical demonstration. In this paper the experimental results are presented of wind tunnel tests with a 1.8m diameter rotor coupled to a water-hydraulic circuit. The goal of the experiments is to prove the functionality of this passive control concept. The components should inherently provide passive torque control for variable speed operation. By sizing the components correctly, the optimal performance of the rotor should be achieved.

The simple arrangement shown in figure 1 was the starting point of the design of the experimental setup. Hydraulic valves were incorporated in order to limit the operational characteristics of the system and keep the components under proper conditions; a pressure relief valve in the high pressure line in order to limit the pressure (in case of overloading) and a closing valve is used to brake the turbine if required. Tap water was used as hydraulic fluid.

2. Theoretical background

2.1. Control of variable speed wind turbines

Modern wind turbines actively manipulate the drive train torque and the pitch angle of the blades to control the aerodynamic performance of the rotor [5]. Between cut-in and rated wind speed the rotor speed is actively controlled using power electronics, with the purpose of maximising energy capture from the wind while keeping the pitch angle constant. Around and above rated wind speed, the blade pitch angle is changed to maintain a constant rotation speed and power up to cut-out wind speed. Figure 2 shows the typical power curve of a variable-speed, variable-pitch wind turbine.

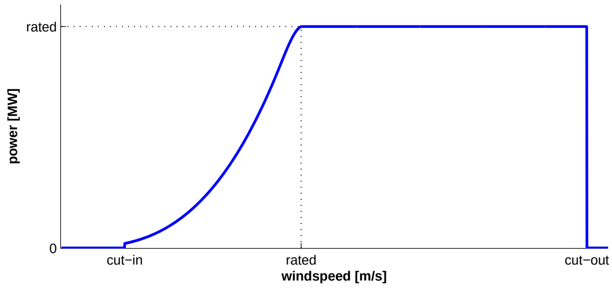

Figure 2. The conventional power curve of an arbitrary variable-speed, variable-pitch wind turbine.

Optimal aerodynamic performance below rated wind speed is possible by maintaining a constant tip speed ratio. The tip speed ratio λ is the ratio between the tangential speed of the blade tip ωR in the rotor plane and the free stream wind speed U_∞.

$$\lambda = \frac{\omega\, R}{U_\infty} \tag{1}$$

This characteristic parameter indicates what the optimal rotation speed ω is for a rotor with radius R at wind speed U_∞. Figure 3(a) shows a typical relation between the tip speed ratio λ, the power coefficient C_P and the torque coefficient C_τ for an aerodynamic rotor at nominal pitch angle β_{nom}. In order to get the maximum power out of the wind, $C_P = C_{P,max}$, the tip speed ratio λ should be at its optimum value. The relation between the power and the torque coefficient is given by the following equation.

$$C_\tau(\lambda, \beta) = \frac{C_P(\lambda, \beta)}{\lambda} \tag{2}$$

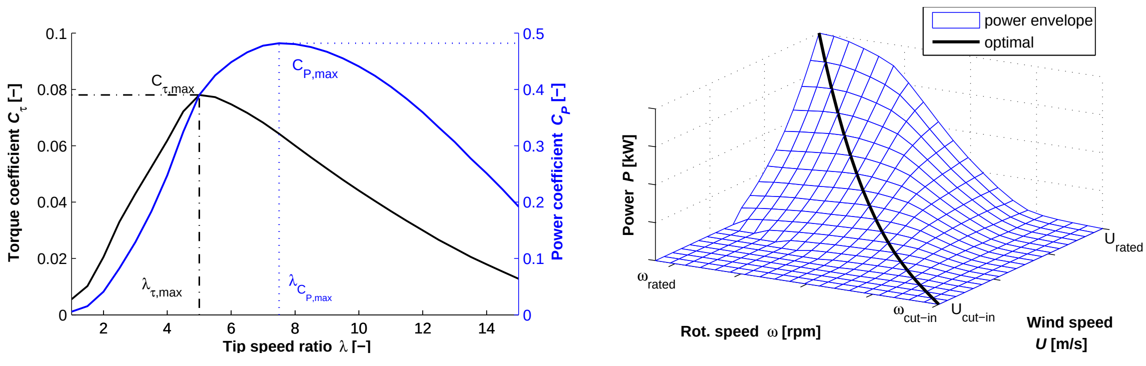

(a) C_P-λ and C_τ-λ performance curves (b) 3D Power curve up to rated wind speed

Figure 3. The aerodynamic performance of an arbitrary variable-speed wind turbine rotor at nominal pitch angle.

2.2. Torque balance at the rotor shaft

Assuming a rigid connection for the rotor-pump assembly and neglecting friction losses, the angular acceleration of the rotor is determined by the balance between the aerodynamic torque τ_{aero} and the drive train torque τ_{pump}. The mass moment of inertia of the rotor-pump assembly is given by I and the air density ρ_{air} is assumed to have constant value.

$$I\,\dot{\omega} = \tau_{aero} - \tau_{pump} \tag{3}$$

$$\tau_{aero} = C_\tau(\lambda,\beta)\,\frac{1}{2}\,\rho_{air}\,U_\infty^2\,\pi R^3 \tag{4}$$

For a fixed pitch angle β, the aerodynamic torque coefficient C_τ is only a function of the tip speed ratio λ, see figure 3(a). Hence for a constant λ, τ_{aero} is directly proportional to U_∞^2. The counter torque produced by the pump with a fixed volumetric displacement V_g is described as a function of the pressure difference across the pump and the mechanical efficiency of the pump η_m.

$$\tau_{pump} = \frac{V_g\,\Delta p}{\eta_m} \tag{5}$$

The pressure difference Δp over the pump is predominantly determined by the actuator at the end of the high pressure line. The flow Q produced by the pump is described as a function of the rotor speed and the volumetric efficiency of the pump η_v.

$$Q = V_g\,\omega\,\eta_v \tag{6}$$

2.3. Euler/Bernoulli's equation for dynamic pressure

Consider a steady, inviscid, incompressible, laminar, unidirectional, one-dimensional flow of a fluid with density ρ through a circular conduit with constant diameter. At the end of the conduit is a nozzle. In the conduit: p_1 is the static pressure and v_1 is the flow speed. At the nozzle outlet: p_2 is the static pressure and v_2 is the flow speed. The relation between pressures and velocities at cross sections 1 and 2 (see figure 4) is given by Bernoulli's equation.

$$p_1 - p_2 = \frac{1}{2}\,\rho\,\left(v_1^2 - v_2^2\right) \tag{7}$$

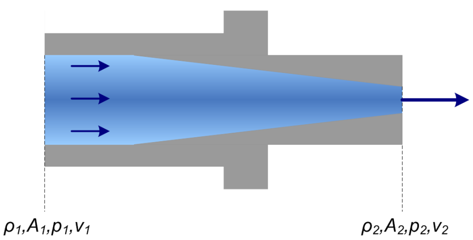

Figure 4. Schematic of the fluid flow through the conduit and the nozzle.

The speed v_2 of the flow out of the nozzle is calculated using the continuity equation. The mass flow $\dot{m}$ on either side of the nozzle outlet is thus in equilibrium.

$$v_1 = \frac{Q}{A_1} \qquad v_2 = \frac{Q}{A_2} \tag{8}$$

2.4. The optimal nozzle outlet diameter

Combining equations 7 and 8, the difference in static pressure inside and outside the conduit is obtained.

$$\Delta p = \frac{1}{2}\rho\, Q^2 \left(\frac{1}{A_2^2} - \frac{1}{A_1^2}\right) \tag{9}$$

The optimal area of the nozzle outlet is calculated by combining equations 1 to 6 and 9, and setting the angular acceleration to zero $\dot{\omega} = 0$. The optimum power extraction corresponds to $C_{P,max}$, which occurs at the optimal tip speed ratio λ_{opt}. This results in expression 10 for the optimal nozzle outlet area A_2.

$$A_2 = \sqrt{\left(\frac{V_g^3\, \lambda_{opt}^3\, \eta_v^2}{C_{P,max}\, \eta_m\, \pi R^5}\right)\left(1 - \frac{A_2^2}{A_1^2}\right)} \tag{10}$$

In reality the values for mechanical and volumetric efficiency will vary slightly depending on the operational conditions. For dimensioning the nozzle however they may be assumed constant for specific design conditions. Hence, each term in equation 10 is a constant. Typically the term $A_2^2/A_1^2 \approx 0$, which allows for a simplification of the equation. Since the nozzle outlet is typically circular, its dimension is hence forth given through its diameter.

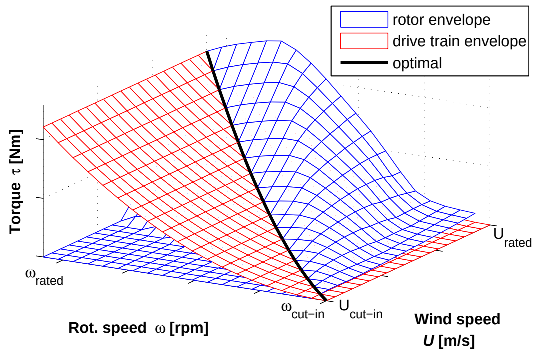

Figure 5. Operational envelopes of the rotor and hydraulic drive train assembly.

The resulting steady state performance envelope of the rotor and drive train is given in figure 5. Here the red area is the envelope of the counter torque produced by the pump, which is a function of the rotation speed only. The drive train torque is directly proportional to the rotation speed squared. The blue area is the rotor torque envelope, which is a function of the tip speed ratio, i.e. both rotation speed and wind speed. The intersection between the red and blue areas marks the region where the system will operate. If the nozzle is dimensioned optimally (as is the case here), this intersection will correspond to the line of optimal performance of the rotor in figure 3(b).

3. Wind tunnel experiments

3.1. Overview of the experimental setup

The passive control concept was validated though wind tunnel experiments with a small horizontal wind turbine in the Open Jet Facility (OJF) at Delft University of Technology. A hydraulic water circuit with different nozzle diameters were tested under a range of wind speeds, resulting in different operational envelopes of the rotor. The hydraulic braking and torque limitation were also tested to prove the functionality of the concept. The hydraulic diagram in figure 6 identifies the essential components of the experimental setup. The main component properties are listed in table 1.

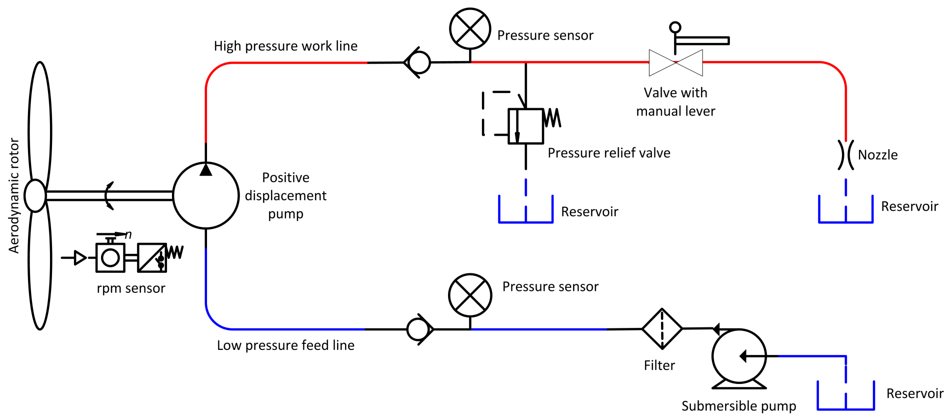

Figure 6. Hydraulic diagram of the experimental setup.

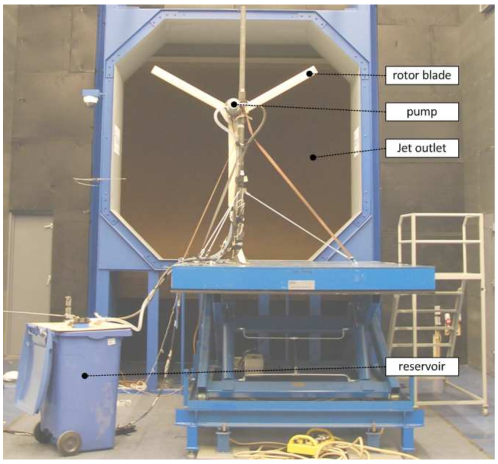

(a) Complete system

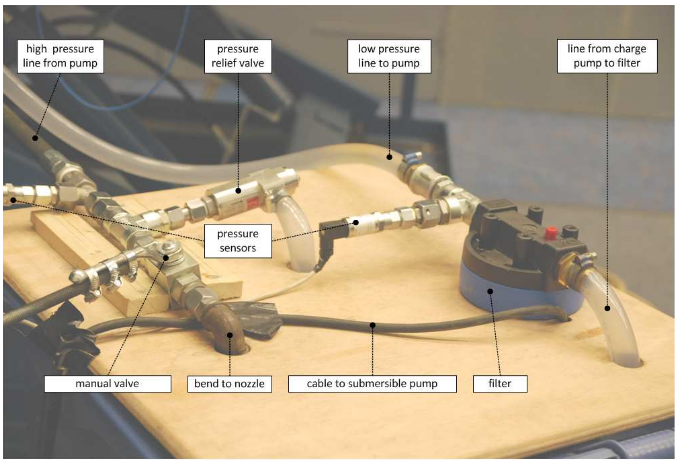

(b) The lid of the water reservoir

Figure 7. Overview of the experimental setup at the Open Jet Facility.

Table 1. Experimental setup component properties.

Component	Properties
Rotor	Diameter: 1.8m, airfoil: NACA 4212
Pump	Danfoss PAH12.5, displacement: 12.5cc/rev
	nominal pressure: 160bar, speed range: 500-1800rpm
Lines	Length: 5m, diameter: 12.5mm (0.5in)
Pressure relief valve	Opening pressure: 35bar
Nozzle	Outlet diameter: 1.24 / 1.32 / 1.35 / 1.42 / 1.51 / 2.07mm

3.2. Experimental results

3.2.1. Steady state results Steady state measurements were done by going from one steady wind speed to the next. A steady state point was logged when the measured air speed out of the OJF remained constant, with a slight variation (turbulence intensity $\approx$ 0.23%), for a few seconds. The result from one measuring sequence versus time is shown in figure 8.

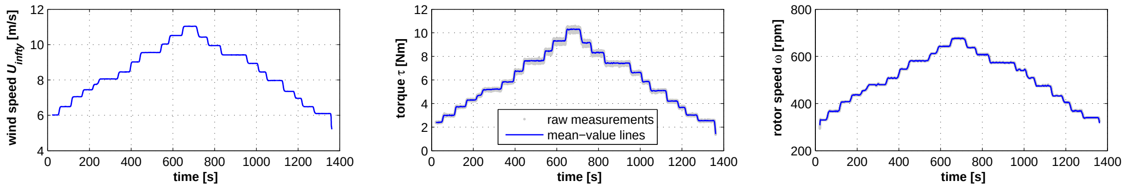

(a) Wind speed (b) Torque (c) Rotor speed

Figure 8. Time series for one continuous run of measurements; horizontal lines indicate steady state.

The measured steady state points for the different nozzle diameters are shown in figure 9(a) and 9(b). The power coefficient of the aerodynamic rotor C_P is given by the following equation.

$$C_P = \frac{\tau\,\omega}{P_{wind}} = \frac{(\Delta p)\;V_g\;\omega\;\eta_v}{\frac{1}{2}\,\rho_{air}\;U_\infty^2\;\pi R^2\;\eta_m} \tag{11}$$

Here V_g and R were known beforehand and ρ_{air}, Δp, ω, U_∞ were measured. The volumetric efficiency η_v of the pump is also accounted, which is around 90% for a wide range of operation. The mechanical efficiency of the pump η_m is unknown, thus the term $C_P\,\eta_m$ gives the overall performance of the system including rotor, bearings and pump.

As seen in figure 9(b), the nozzle diameter D_{nozzle} = 1.32mm proved to yield a drive train torque that resulted in rotor operation with the highest performance. Under ideal circumstances, assuming incompressible flow and an ideal pump, the steady state value of $C_P\eta_m$ in figure 9(b) would be constant throughout the displayed range of rotational speeds. Above 500rpm the perfromance still increase, but only marginally. However, for decreasing wind speed and rotational speed, the measurements and related trend lines in the figure show a deviation from this expected constant value due to the low mechanical efficiency. Two causes are attributed to this phenomenon:

(i) The internal friction in the pump cylinders has a significant effect on effective braking torque at low rotational speeds (ω < 500rpm). This is seen in the relatively high value of the required start-up torque of 4Nm for the Danfoss PAH12.5 pump.

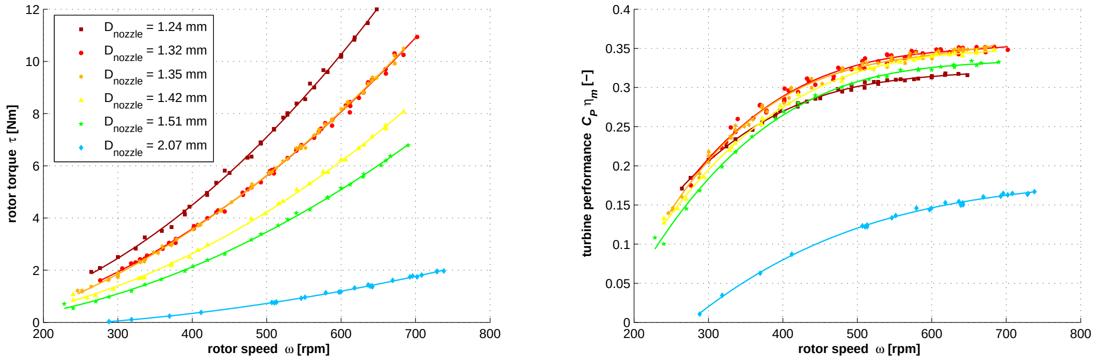

(a) Torque-speed relations (b) Performance comparison

Figure 9. Steady-state results of the OJF measurements for different nozzles.

(ii) The Reynolds number at low wind speeds is small enough for viscous friction to play a significant role. The effect of this phenomenon is minimal for large wind turbines simply because of the greater rotor diameter. This is also noted in [6].

3.2.2. Transient results A "transient" here refers to the transition between steady state points, as is indicated in figure 10. For the presentation of the transient results, the case where $D_{nozzle} = 1.32$mm is taken.

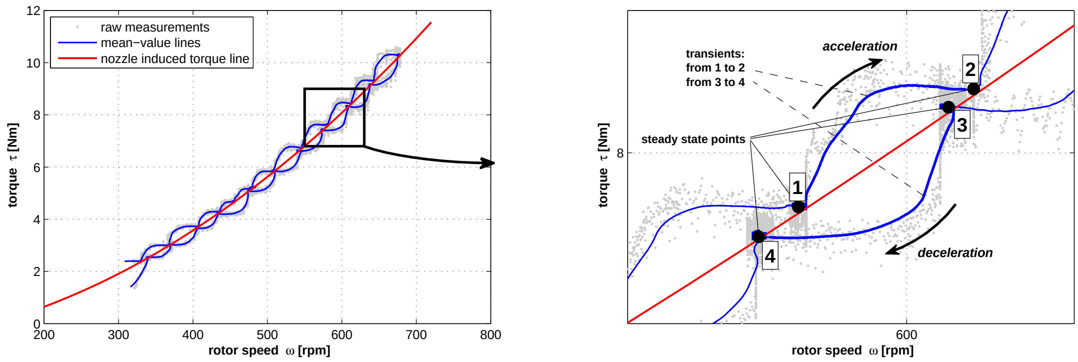

(a) Transient results of one time series measurements (b) Zoomed-in results

Figure 10. Steady state and transients explained for the torque-speed curve, corresponding to the time series with $D_{nozzle} = 1.32$mm.

The results in figure 11 show the operation of the rotor around the intersection between the rotor envelope and the drive train envelope. The data around the intersection displays a pattern of bends. These are explained by the experimentation sequence. After start-up, the wind speed was increased from point to point until a certain maximum (10-12m/s) and again decreased along the same points, to yield multiple "steady state" measurements for the same wind speed. The data in between the "steady state" points forms the bends. The bend above the intersection indicates the torque and speed transition to a higher wind speed. The lower bends result from a decrease in wind speed. This shows that for a change in wind speed, the torque always balances along the intersection of envelopes.

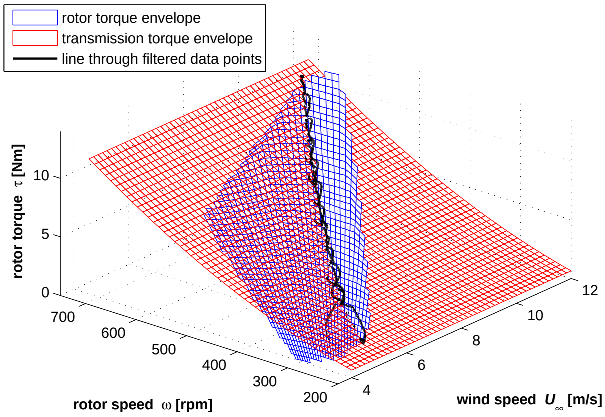

Figure 11. The measured transient response mapped onto the measured operational envelopes of the rotor and the fluid power transmission.

3.2.3. Limiting the drive train torque through the pressure relief valve For the purpose of general safety, every hydraulic circuit should have one or more pressure relief valves. These valves are set to open when the pressure p reaches a predetermined threshold p_{lim}. Thus, the effect of the pressure relief valve is that it sets the limit for the maximum torque. For a conventional drive train, the maximum torque is set by the power electronics. At high wind speeds, overspeed of the rotor due to the surplus of aerodynamic torque over the drive train torque is prevented through pitch control, i.e. manipulating the pitch angle of the rotor blades.

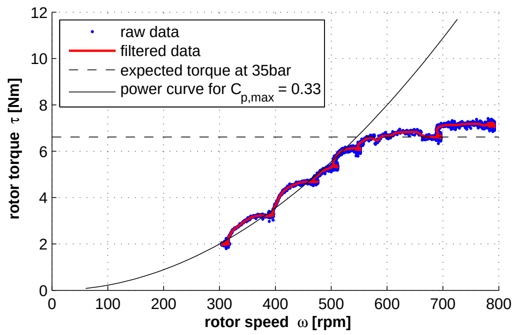

Figure 12. Transient response for drive train torque limitation using a pressure relief valve.

To demonstrate the torque limitation on the experimental setup, the pressure relief valve was adjusted to open at around 35 bar. The response of the system is shown in figure 12. The significance of this demonstration is that such a simple and highly reliable component is able to limit the pressure and torque to a preset maximum. Thus, by setting the activation pressure of the relief valve correctly, the torque envelope of the hydraulic drive train is rendered in a similar way as for an electrically controlled drive train, but with a simpler and far less expensive components.

3.2.4. Emergency shutdown function: hydraulic braking results The rotor speed of a wind turbine should be able to stop if a shut down is demanded during operation. The requirements for an emergency stop are given in [7]. Three independent ways to stop a wind turbine from rotating are:

(i) pitching the blades to decrease the aerodynamic torque.
(ii) yawing the rotor out of the wind.
(iii) increasing the transmission torque.

Increasing the transmission torque is possible using a valve across the high pressure line. When the valve is being closed the pressure in the system builds up, essentially in the same way as the nozzle induces pressure. The required rotor torque thus increases and the rotor slows down.

Looking at the C_τ curve in figure 3(a), the point of operation thus moves from the point in line with $C_{P,max}$ to the left up to the point $C_{\tau,max}$. This point marks the border between stable and unstable operation. To the left of this point, $C_{\tau,max}$ value drops rapidly; the torque that is required from the rotor by the transmission cannot be matched and the rotor will slow to a stop.

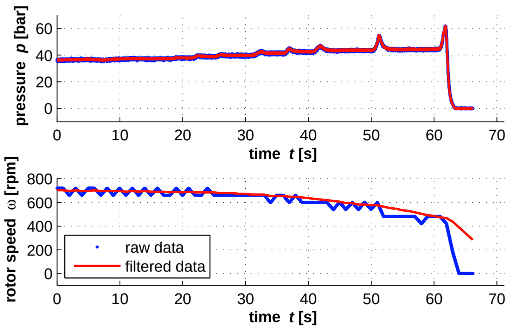

Figure 13. Transient response for hydraulic braking: the results from gradually closing the manual valve located before the nozzle (indicated in figures 6 and 7(b)).

The experiments to prove hydraulic braking were done using a manual valve. The initial condition is a steady state operation, meaning constant rotor speed, torque and wind speed. The measurement results in figure 13 show how the pressure (and thus torque) gradually builds up and the rotor speed slows down as the manual valve is slowly closed. Once the threshold corresponding to $C_{\tau,max}$ is reached the rotor rapidly comes to a halt.

The hydraulic braking can be done at any point along the high pressure line(s) of the fluid power transmission. Although many configurations are possible, the simplest is to have a second relief valve with a much higher threshold pressure upstream of the manual shutting valve and the torque limiting pressure relief valve down stream. In contrast to a mechanical brake, a hydraulic brake is continuously operable, because it loses heat through the hydraulic fluid.

4. Conclusion & Outlook

The results of wind tunnel experiments show that it is possible to implement a passive control for variable speed rotors using fluid power technology. A small rotor coupled to a water-hydraulic circuit was used to demonstrate the working principle of the proposed concept.

The torque envelope of a conventional variable speed wind turbine drive train can be achieved for the hydraulic transmission through solely passive control. For operation below rated wind speeds, the drive train torque-speed envelope is matched closely to the optimal aerodynamic curve of the rotor by optimally sizing the constant cross-sectional area of the nozzle. Above rated wind speed a pressure relief valve is activated in order to limit the pressure and consequently the drive train torque. A method for shutting down the turbine using the hydraulic drive train was also presented. The wind turbine rotor is stopped by gradually cutting off the volumetric flow rate in the high pressure line by means of a valve.

The passive torque control showed an inherently stable operation for all nozzles used in these experiments. However for a different rotor, pump or hydraulic fluid, it is important to consider the drive train parameters which might have an influence in the system response; a drive train with lower stiffness is expected for a large volume of fluid and/or lower fluid compressibility.

Another important consideration is the overlapping of the rotor rotation frequencies with the resonance frequencies of the support structure. During the experiments it was observed that around 460rpm the rotation speed matched a resonance frequency of the support structure. The wind speed corresponding to this rotor speed, which is different for every nozzle, was skipped to avoid damage to the setup.

Specifically for the conducted experiments it was found that the effect of hydraulic losses is minimal at pump rotation speeds greater than 500rpm. The pump used in the experiments was not designed for speeds below 500rpm. Its start-up torque makes it unsuited for this type of application outside of a test environment.

The presented and proven concept of passive torque control could lead to innovations in other wind energy technologies such as water desalination and water pumping applications where the need of converting wind energy into electricity is eliminated. In June 2012 patent request P31185NL00/MVE was filed by the TU Delft for this control method.

Acknowledgements

We thank Nico van Beek, Nando Timmer, Ruud van Rooij, Joost Sterenborg and Nienke Hosman for their help with the experiments at the Open Jet Facility of the TU Delft.

References

[1] Salter S H and Rea M 1984 *Hydraulics for wind* European Wind Energy Conference (Hamburg: EWEA) pp 534-541

[2] Schmitz J, Diepeveen N, Vatheuer N and Murrenhoff H 2011 *Dynamic transmission response of a hydrostatic transmission measured on a test bench* European Wind Energy Conference (Brussels: EWEA) pp 197-206

[3] Diepeveen N 2013 *On Fluid Power Transmission for Offshore Wind Turbines* PhD Thesis (Delft: Technical University of Delft)

[4] Chapple P, Niss M and Thomsen K E 2012 *Wind turbines with variable hydraulic transmissions and electrically excited synchronous generators directly connected to the grid* Fluid Power and Motion Control Symposium ed D N Johnston and A R Plummer (Bath: Centre for Power Transmission and Motion Control) pp 579-592

[5] Bianchi F D, Battista H and Mantz R J 2009 *Wind Turbine Control Systems: Principles, Modelling and Gain Scheduling Design* Advances in Industrial Control (London: Springer)

[6] Hosman N 2012 *Performance analysis and improvement of a small locally produced wind turbine for developing countries* MSc Thesis (Delft: Technical University of Delft)

[7] International Standard 2005 *IEC 61400-1 Ed.3: Wind turbines - Part 1: Design requirements:Design requirements* Reference number IEC 61400-1:2005(E)